

## Displacement of a bubble located at a fluid-viscoelastic medium interface

Hasan Koruk, and James J. Choi

Citation: [The Journal of the Acoustical Society of America](#) **145**, EL410 (2019); doi: 10.1121/1.5108678

View online: <https://doi.org/10.1121/1.5108678>

View Table of Contents: <https://asa.scitation.org/toc/jas/145/5>

Published by the [Acoustical Society of America](#)

---

---

GCRIIS



CAPTURE WHAT'S POSSIBLE  
WITH OUR NEW PUBLISHING ACADEMY RESOURCES

Learn more 



# Displacement of a bubble located at a fluid-viscoelastic medium interface

Hasan Koruk<sup>a)</sup>

Mechanical Engineering Department, MEF University, Istanbul 34396, Turkey  
korukh@mef.edu.tr

James J. Choi

Department of Bioengineering, Imperial College London, London SW7 2AZ,  
United Kingdom  
j.choi@imperial.ac.uk

**Abstract:** A model for estimating the displacement of a bubble located at a fluid-viscoelastic medium interface in response to acoustic radiation force is presented by extending the model for a spherical object embedded in a bulk material. The effects of the stiffness and viscosity of the viscoelastic medium and the amplitude and duration of the excitation force on bubble displacement were investigated using the proposed model. The results show that bubble displacement has a nonlinear relationship with excitation duration and viscosity. The time at which the steady state is reached increases with increasing medium viscosity and decreasing medium stiffness.

© 2019 Acoustical Society of America

[JT]

Date Received: February 4, 2019

Date Accepted: April 29, 2019

## 1. Introduction

Ultrasound has been used to determine tissue properties, such as the elastic modulus (Ophir *et al.*, 1991; Fatemi and Greenleaf, 1998; Sarvazyan *et al.*, 2010). More recently, the use of microbubbles in a fluid to push against tissue under ultrasound exposure was proposed to improve the contrast and spatial resolution of elasticity imaging (Koruk *et al.*, 2015). There are several mathematical models that exist for bubbles exposed to sound in a liquid (Prosperetti, 1987; Church, 1995; Doinikov *et al.*, 2009; Marmottant *et al.*, 2005) or in an elastic and viscoelastic medium (Yang and Church, 2005; Zabolotskaya *et al.*, 2005; Barajas and Johnsen, 2017). Furthermore, there are some models for the displacement of a bubble completely embedded in a tissue (Ilinskii *et al.*, 2005; Chen *et al.*, 2002; Aglyamov *et al.*, 2007; Karpiouk *et al.*, 2009; Urban *et al.*, 2011; Yoon *et al.*, 2011; Mikula *et al.*, 2014). However, the displacement of a bubble located at a fluid-viscoelastic medium interface has not been comprehensively explored in the literature.

In the therapeutic and diagnostic ultrasound applications that use microbubbles, a large proportion of bubbles will be located at fluid-tissue interfaces (Erpelding *et al.*, 2005; Doherty *et al.*, 2013; ter Haar, 2007; Acconcia *et al.*, 2013; Pouliopoulos *et al.*, 2018). In a previous study, we developed a mathematical model for the displacement of a bubble located at a fluid-elastic medium interface in response to acoustic radiation force (Koruk and Choi, 2018). However, besides the elasticity, the viscosity of a tissue can significantly affect the dynamic response (Kruse *et al.*, 2000; Yoon *et al.*, 2011). Therefore, in the present study, a mathematical model for the displacement of a bubble located at a fluid-viscoelastic medium interface, which more accurately simulates the practice, was developed.

The technique for modelling the displacement of a bubble followed in this study is based on the approach used for the displacement of a spherical object embedded in a bulk material (Ilinskii *et al.*, 2005; Yoon *et al.*, 2011) and the mathematical model proposed for a bubble located at a fluid-elastic medium interface (Koruk and Choi, 2018). However, as in practice, the medium was modelled to exhibit both the elastic and viscous characteristics this time. In addition, after the validity of the model was briefly evaluated, the effects of the stiffness and viscosity of the viscoelastic medium and the amplitude and duration of the excitation force on bubble displacement were explored using the proposed model. Since the microbubbles used in

<sup>a)</sup>Author to whom correspondence should be addressed.

biomedical ultrasound applications are frequently located at fluid-viscoelastic medium interfaces, our model can be exploited in practical applications including the determination of the stiffness of tissue microenvironments.

### 2. Mathematical model

A bubble at fluid-solid interface [Fig. 1(a)] displaces the surrounding medium when it is exposed to an external force [Fig. 1(b)]. Here, it is assumed that the surrounding environment is homogeneous and isotropic (Yoon *et al.*, 2011). The medium is assumed to be incompressible, as it is in most tissues (Yoon *et al.*, 2011; Sarvazyan, 1975). The model for the medium material includes both elastic and viscous characteristics (i.e., the medium is modeled as a viscoelastic material), as in practice (Yoon *et al.*, 2011; Sarvazyan, 1975; Zhou *et al.*, 2017; Maccabi *et al.*, 2018). It is assumed that the medium does not rupture. The fluid dynamic properties, such as fluid inertia are ignored (Field and Drzewiecki, 1998). It should be noted that the acoustic impedance mismatch between the bubble and the surrounding fluid or tissue is much greater than the mismatch between the fluid and the tissue. Therefore, the contribution of the radiation force due to the acoustic impedance mismatch between the fluid and the viscoelastic medium is neglected. The problem here is axisymmetric and there is no force dependence in the azimuthal direction. Therefore, the deformation of the bubble is symmetrical about the  $x$  axis. The equation of motion for incompressible viscoelastic medium in time domain is given by (Yoon *et al.*, 2011)

$$-\nabla p + G\nabla^2 \mathbf{u} + \eta \nabla^2 \frac{\partial \mathbf{u}}{\partial t} = \rho \frac{\partial^2 \mathbf{u}}{\partial t^2}, \tag{1}$$

where  $p$  is the internal pressure;  $\mathbf{u}$  is the displacement vector;  $G$ ,  $\eta$ , and  $\rho$  are the shear modulus, viscosity, and density of the medium, respectively; and  $t$  shows the time.

The polar axis of the spherical system of coordinates  $(r, \theta, \phi)$  is along the force vector (i.e., there is an angle  $\theta$  between the radius vector and displacement) and the vector of displacement due to an external force  $f_e$  has radial ( $u_r$ ) and polar ( $u_\theta$ ) components given by  $\mathbf{u} = (u_r, u_\theta, 0)$ . For the problem illustrated in Fig. 1, the external force applied to a displaced bubble can be written as (Koruk and Choi, 2018)

$$f_e = -2\pi R^2 \int_0^{\theta_h} (\sigma_{rr} \cos \theta - \sigma_{r\theta} \sin \theta) \sin \theta d\theta, \tag{2}$$

where  $R$  is the radius of the bubble and  $\theta_h$  is the angle between the  $x$ -axis and  $r$ -axis corresponding to the displacement  $h$ . Here  $\sigma_{rr}$  and  $\sigma_{r\theta}$  show the components of stress tensor at the surface of the bubble. The boundary conditions at the bubble surface (i.e., at  $r = R$ ) can be written as

$$-\sigma_{rr} + p_e = p_g, \quad \sigma_{r\theta} = 0, \tag{3}$$

where  $p_e$  is the pressure acting on the bubble surface (i.e., acoustic radiation pressure) and  $p_g$  is the internal gas pressure. Here, we consider an external force with an amplitude  $f_0$  and a finite length  $\tau$  given by

$$f_e = \begin{cases} f_0, & 0 \leq t \leq \tau, \\ 0, & t > \tau. \end{cases} \tag{4}$$

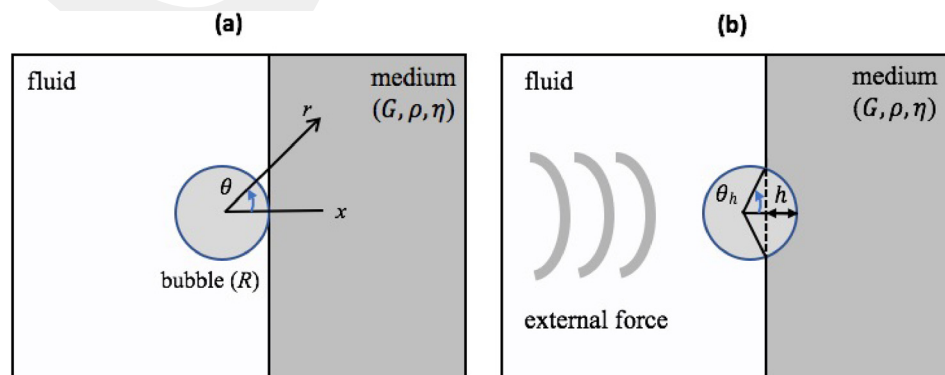


Fig. 1. (Color online) The bubble (with the radius  $R$ ) located at fluid-solid interface (a) displaces the surrounding medium (with the shear modulus  $G$ , density  $\rho$ , and viscosity  $\eta$ ) when it is exposed to an external force (b).

By substituting the expressions for the relation between the external pressure  $p_e$  and force  $f_e$  (Koruk and Choi, 2018) and the stress tensor components (Yoon *et al.*, 2011) into Eq. (3), we can obtain the solution as follows:

$$u_r = -\frac{jf_0}{6\pi R \left[1 - \left(1 - \frac{u_{r0}}{R}\right)\right]} \mathcal{F}^{-1} \left[ \frac{(e^{j\omega\tau} - 1)(3 - jkR)}{\omega(G - j\eta\omega) \left(1 - jkR - \frac{1}{6}k^2R^2 + \frac{1}{18}jk^3R^3\right)} \right] \cos \theta, \quad (5)$$

$$u_\theta = \frac{jf_0}{12\pi R \left[1 - \left(1 - \frac{u_{r0}}{R}\right)\right]} \mathcal{F}^{-1} \left[ \frac{(e^{j\omega\tau} - 1)(3 + jkR)}{\omega(G - j\eta\omega) \left(1 - jkR - \frac{1}{6}k^2R^2 + \frac{1}{18}jk^3R^3\right)} \right] \sin \theta, \quad (6)$$

where  $k$  is the wave number of the shear wave with the frequency  $\omega$ ,  $u_{r0}$  is the radial displacement component for  $\theta = 0$ , and  $\mathcal{F}^{-1}$  represents the inverse Fourier transform. For a given force  $f_0$ , specific time  $t$  and  $\theta = 0$ , the unknown  $u_{r0}$  in Eq. (5) can be determined. Here, the excitation duration  $\tau$  was divided into  $N$  (e.g., 100) points and the calculations were repeated over the entire time period of interest using MATLAB (Mathworks, Natick, MA). Once  $u_{r0}$  is determined, the radial and polar displacement components for any  $\theta$  can be determined using Eqs. (5) and (6). It should be noted that we used the minimum ( $\approx -10^{309}$ ) and maximum ( $\approx 10^{309}$ ) numbers defined in MATLAB for the evaluation of the integrals in Eqs. (5) and (6). It is believed that the model presented here can simulate the practice appropriately and the model can be improved further by taking the surface tension and bubble oscillatory dynamics into account in the model. The use of different bubble models, including surface tension and radial and translational oscillatory bubble dynamics (Watanabe and Kukita, 1993; Zheng *et al.*, 2007; Mettin and Doynikov, 2009), will be considered in our future studies.

### 3. Methods

The shear modulus for a tissue-mimicking material with a viscosity of 0.7 Pa s was determined to be around 6.5 kPa using an indentation test where a sphere with a radius of 4 mm was used (Qiang *et al.*, 2011). In this test, a maximum displacement of 0.96 mm was obtained for the force amplitude of 75 mN. Assuming that the maximum displacements for a bubble and sphere (Ilinskii *et al.*, 2005) will be the same for this case, our model for this displacement estimates that the shear modulus of the material is about 5.5 kPa (i.e., our model predicts that the maximum displacement of a bubble with a radius of 4 mm is 0.96 mm when the shear modulus is set to 5.5 kPa). It should be noted that, to the best knowledge of the authors, no prior study has presented experimental displacement-force relationship for a bubble located at a fluid-viscoelastic medium interface. Although the indirect comparison here helps to evaluate the validity of the proposed model, experimental investigation using small and large bubbles (e.g., 1–200  $\mu\text{m}$  in radius) at fluid-viscoelastic material (e.g., gelation with different concentrations) interfaces and different ultrasound parameters (e.g., sonication frequency and pulse length) will be considered in our future studies.

In the following, we explored the effects of the stiffness and viscosity of the medium and the amplitude and duration of the excitation force on bubble displacement using the proposed model. Analyses are performed for physiologically relevant materials (i.e.,  $G = 2\text{--}4\text{ kPa}$ ,  $\rho = 1000\text{ kg/m}^3$ , and  $\eta = 0.02\text{--}2\text{ Pa s}$ ). For example, the shear modulus, density and viscosity of the liver are around 2 kPa (Maccabi *et al.*, 2018), 1000 kg/m<sup>3</sup> (Woodard and White, 1986), and 0.5 Pa s (Chen *et al.*, 2009), respectively. It should be noted that in small vessels, such as arterioles and capillaries, their thickness approaches a single cell and in the case of microvessels with thin walls, the vessel takes on the elasticity of the surrounding tissue microstructures (Saharkhiz *et al.*, 2018). Therefore, the model presented here can be used to determine the stiffness of tissue microenvironments. It should be remembered that the microbubbles typically range from 0.5 to 5  $\mu\text{m}$  in radius (Postema and Gilja, 2011; Appis *et al.*, 2015). The mean radii were reported to be 0.55–1.65 and 1.5–2.25  $\mu\text{m}$  (Karshafian *et al.*, 2010), respectively, for the commercially available microbubbles Definity<sup>®</sup> and Optison<sup>®</sup>. It should be noted that large bubbles (i.e.,  $R = 25\text{--}250\text{ }\mu\text{m}$ ) are frequently used in research to identify the mechanical properties of materials and explore bubble dynamics (Erpelding *et al.*, 2005; Yoon *et al.*, 2011). The analyses are performed for both small and large bubbles (i.e.,  $R = 2\text{--}100\text{ }\mu\text{m}$ ) in this study. The magnitude of the acoustic

radiation force on a bubble with a diameter of  $1\ \mu\text{m}$  is determined to be  $5\ \text{nN}$  when the peak negative pressure is  $100\ \text{kPa}$  and the excitation frequency is  $2.25\ \text{MHz}$  (Dayton *et al.*, 2002). The magnitude of excitation force produced on bubbles increases as the bubble diameter increases and it can be in the order of  $\mu\text{Ns}$  for larger bubbles even when the excitation frequency is far from the resonance frequency of the bubble (Dayton *et al.*, 2002; Leighton *et al.*, 1990). The magnitude of excitation force is chosen as  $2.5\text{--}25\ \text{nN}$  for small bubbles (i.e.,  $R=2\text{--}4\ \mu\text{m}$ ) and  $10\ \mu\text{N}$  for the large bubble (i.e.,  $R=100\ \mu\text{m}$ ) in this study. It should be noted that it was shown that the bubble remains almost spherical when bubble displacement does not exceed half times the radius of the bubble for medium materials with similar elastic properties studied in this paper (Ilinskii *et al.*, 2005; Koruk and Choi, 2018).

#### 4. Results and discussion

The time response of a bubble ( $R=100\ \mu\text{m}$ ) at a fluid-medium ( $G=2\ \text{kPa}$  and  $\rho=1000\ \text{kg/m}^3$ ) interface with different medium viscosities ( $\eta=0.02, 0.05, 0.10,$  and  $0.25\ \text{Pa s}$ ) and an external force ( $f_0=10\ \mu\text{N}$ ) with different durations ( $\tau=10, 30, 100,$  and  $300\ \mu\text{s}$ ) in Fig. 2 clearly show that viscosity dramatically changes the displacement profile. Oscillatory behaviour is observed in bubble displacement for small viscosity values [Fig. 2(a)] while there are no oscillations when the viscosity is high enough [Figs. 2(b)–2(d)]. This is expected because the damping force slows the back and forth motion and, when the viscosity force is large enough, the medium does not oscillate (i.e., move toward the equilibrium). It is seen that a minimum excitation duration to reach the steady state is required (e.g., around  $300\ \mu\text{s}$  for  $\eta=0.02\ \text{Pa s}$ ).

The maximum displacements for a microbubble ( $R=3\ \mu\text{m}$ ) and different medium ( $G=2\ \text{kPa}$  and  $\rho=1000\ \text{kg/m}^3$ ) viscosities ( $\eta=0.03, 0.10, 0.40,$  and  $2.0\ \text{Pa s}$ ) as a function of the duration of the excitation force ( $f_0=25\ \text{nN}$ ) in Fig. 3(a) clearly show that the bubble displacement has a nonlinear relation with the excitation duration. For a highly damped medium, the steady-state displacement can be achieved by keeping the excitation duration long enough. For example, the time duration to reach to the steady state for the system in Fig. 3(a) is  $0.13, 0.38, 1.65,$  and  $9.0\ \text{ms}$  for  $\eta=0.03, 0.10, 0.40,$  and  $2\ \text{Pa s}$ , respectively. It is seen that when the pulse duration gets close to the values that induce the steady state displacement, the increase in maximum bubble displacement decreases slowly. The results ( $R=3\ \mu\text{m}, G=2\ \text{kPa}, 1000\ \text{kg/m}^3,$  and  $f_0=25\ \text{nN}$ ) for different excitation durations ( $\tau=0.1, 0.2, 0.4,$  and  $0.8\ \text{ms}$ ) in Fig. 3(b) clearly show the nonlinear effect of the medium viscosity on the bubble displacement. The bubble displacement decreases nonlinearly as viscosity increases for a specific excitation duration. For example, the bubble displacement is  $0.95, 0.88,$  and  $0.74\ \mu\text{m}$  for  $\eta=0.5, 1.0,$  and  $2.0\ \text{Pa s}$ , respectively, when  $\tau=0.8\ \text{ms}$ .

The response of a microbubble ( $R=2\ \mu\text{m}$ ) for two different medium ( $\eta=0.25\ \text{Pa s}$  and  $\rho=1000\ \text{kg/m}^3$ ) moduli ( $G=2$  and  $4\ \text{kPa}$ ) excited for  $\tau=1\ \text{ms}$  with different force amplitudes ( $f_0=2.5, 5, 10,$  and  $20\ \text{nN}$ ) as a function of time in Fig. 4 shows that the force magnitude does not change the time at which the steady state is reached.

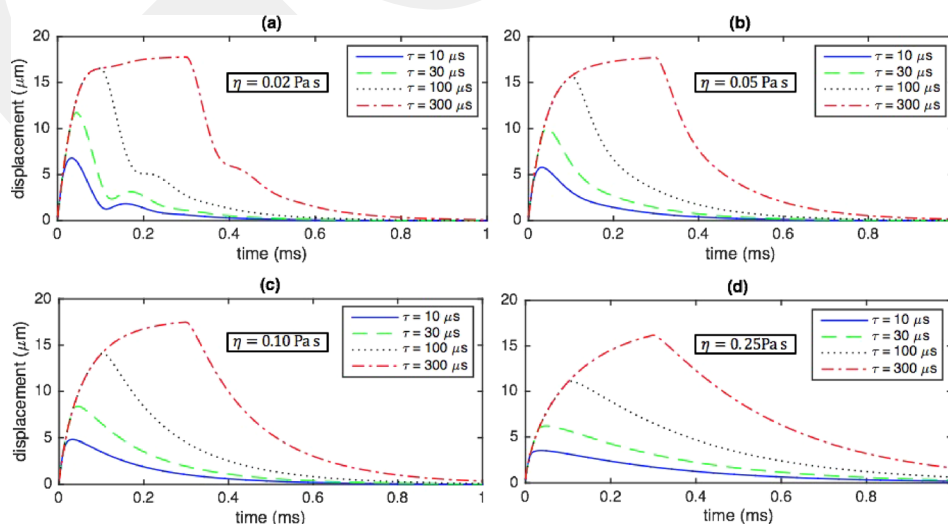


Fig. 2. (Color online) The response of a bubble ( $R=100\ \mu\text{m}$ ) for a medium ( $G=2\ \text{kPa}$  and  $\rho=1000\ \text{kg/m}^3$ ) with the viscosity ( $\eta$ ) of (a)  $0.02$ , (b)  $0.05$ , (c)  $0.10$ , and (d)  $0.25\ \text{Pa s}$  and an external force with the amplitude of  $f_0=10\ \mu\text{N}$  and different pulse durations ( $\tau=10, 30, 100,$  and  $300\ \mu\text{s}$ ).

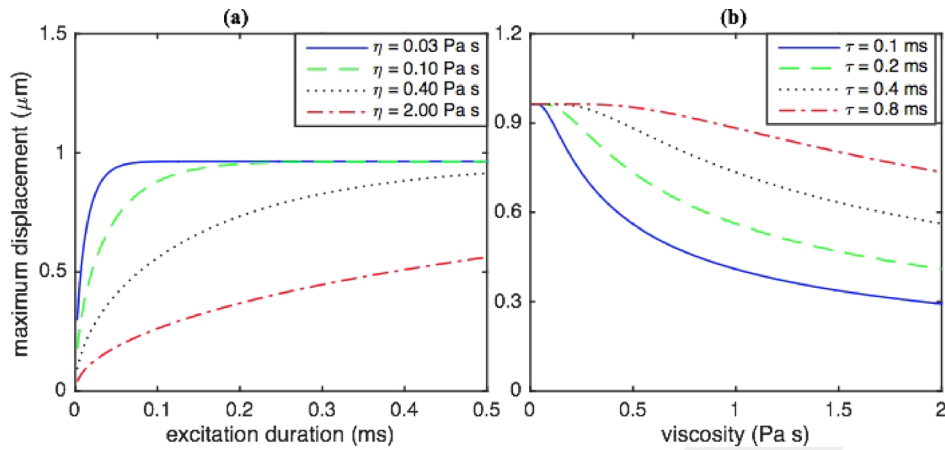


Fig. 3. (Color online) The change of the displacement of a microbubble ( $R = 3 \mu\text{m}$ ) at the fluid-medium ( $G = 2 \text{ kPa}$  and  $\rho = 1000 \text{ kg/m}^3$ ) interface: (a) for different medium viscosities ( $\eta = 0.03, 0.10, 0.40,$  and  $2.0 \text{ Pa s}$ ) as a function of the duration of the excitation force ( $f_0 = 25 \text{ nN}$ ), and (b) for different excitation force ( $f_0 = 25 \text{ nN}$ ) durations ( $\tau = 0.1, 0.2, 0.4,$  and  $0.8 \text{ ms}$ ) as a function of medium viscosity.

However, the time to reach steady state depends on the medium stiffness; the medium with a high shear modulus responds faster. For example, for all force levels, the steady state is revealed at about 0.9 and 0.5 ms for  $G = 2$  and 4 kPa, respectively. Please note that 0.9 and 0.5 ms correspond to 450 and 250 cycles of an ultrasound plane wave, for example, if the excitation frequency is 0.5 MHz. It should be noted that the oscillatory behaviour of the excitation force is neglected here; the same has been done previously (Yoon *et al.*, 2011).

It is seen that the model presented here can provide an explanation for the dynamic response of a bubble at a fluid-viscoelastic medium interface exposed to an external force. The model can be exploited in practical applications. It can be used to understand the measured echo signal from a bubble at a fluid-medium interface under ultrasound exposure. The stiffness of tissue microenvironments can be determined by measuring the response of the bubble under ultrasound exposure and the formulation presented here. It can be used to design experiments, for example, to select the excitation duration for a specific bubble displacement when the microbubble radius and material properties are approximately known. We have presented the model for the displacement of a single bubble located at a fluid-viscoelastic medium interface in this study, though many microbubbles will be flowing throughout the vessels in biomedical applications. However, microbubbles injected into the blood at the clinical dose will likely be isolated from each other. Although the distance between the microbubbles may vary locally, a clinical dose of microbubbles ( $c = 2 \times 10^6$  microbubbles/ml), based on rough calculations using  $L = c^{-1/3}$  (Kryuchkov, 2001; Lazarus *et al.*, 2017), will result in a mean inter-bubble distance of  $L = 80 \mu\text{m}$ , noting that the microbubbles typically range from 0.5 to 5 μm in radius (Postema and Gilja, 2011; Appis *et al.*, 2015). Here, we assumed that there is no tissue rupture or any long-term alteration to the tissue stiffness, though this should be investigated experimentally in the future. Experimental investigation using large and small isolated bubbles and many

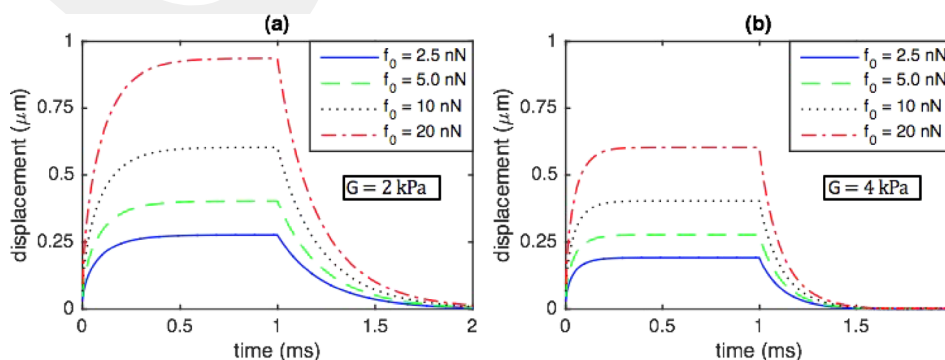


Fig. 4. (Color online) The response of a microbubble ( $R = 2 \mu\text{m}$ ) for a medium ( $\eta = 0.25 \text{ Pa s}$  and  $\rho = 1000 \text{ kg/m}^3$ ) with the shear modulus ( $G$ ) of (a) 2 and (b) 4 kPa excited for  $\tau = 1 \text{ ms}$  with different force levels ( $f_0 = 2.5, 5, 10,$  and  $20 \text{ nN}$ ).

microbubbles flowing in a channel exposed to ultrasound as well as the improvement of the model by taking the surface tension and bubble oscillatory dynamics into account will be considered in our future studies.

## 5. Conclusion

In this study, we developed a mathematical model for the displacement of a bubble at a fluid-viscoelastic medium interface in response to acoustic radiation force by extending the model for a spherical object embedded in a bulk material. We investigated the effects of the stiffness and viscosity of the medium and the amplitude and duration of the excitation force on bubble displacement using the proposed model. The results show that the bubble displacement has a nonlinear relation with the excitation duration and the medium stiffness and viscosity. The time at which the steady state is reached increases with increasing medium viscosity and decreasing medium stiffness. The potential applications of the model presented in this study include the determination of the stiffness of tissue microenvironments, as the bubbles used in biomedical ultrasound applications are frequently found at fluid-viscoelastic medium interfaces.

## References and links

- Acconcia, C., Leung, B. Y. C., Hynynen, K., and Goertz, D. E. (2013). "Interactions between ultrasound stimulated microbubbles and fibrin clots," *Appl. Phys. Lett.* **103**, 053701.
- Aglyamov, S. R., Karpouk, A. B., Ilinskii, Y. A., Zabolotskaya, E. A., and Emelianov, S. Y. (2007). "Motion of a solid sphere in a viscoelastic medium in response to applied acoustic radiation force: Theoretical analysis and experimental verification," *J. Acoust. Soc. Am.* **122**, 1927–1936.
- Appis, A. W., Tracy, M. J., and Feinstein, S. B. (2015). "Update on the safety and efficacy of commercial ultrasound contrast agents in cardiac applications," *Echo Res. Pract.* **2**(2), R55–R62.
- Barajas, C., and Johnsen, E. (2017). "The effects of heat and mass diffusion on freely oscillating bubbles in a viscoelastic, tissue-like medium," *J. Acoust. Soc. Am.* **141**, 908–918.
- Chen, S., Fatemi, M., and Greenleaf, J. F. (2002). "Remote measurement of material properties from radiation force induced vibration of an embedded sphere," *J. Acoust. Soc. Am.* **112**, 884–889.
- Chen, S., Urban, M. W., Pislaru, C., Kinnick, R., Zheng, Y., Yao, A., and Greenleaf, J. F. (2009). "Shearwave dispersion ultrasound vibrometry (SDUV) for measuring tissue elasticity and viscosity," *IEEE Trans. Ultrason. Ferroelectr. Freq. Control* **56**, 55–62.
- Church, C. C. (1995). "The effects of an elastic solid surface layer on the radial pulsations of gas bubbles," *J. Acoust. Soc. Am.* **97**, 1510–1521.
- Dayton, P. A., Allen, J. S., and Ferrara, K. W. (2002). "The magnitude of radiation force on ultrasound contrast agents," *J. Acoust. Soc. Am.* **112**, 2183–2192.
- Doherty, J., Trahey, G., Nightingale, K., and Palmeri, M. (2013). "Acoustic radiation force elasticity imaging in diagnostic ultrasound," *IEEE Trans. Ultrason. Ferroelectr. Freq. Control* **60**, 685–701.
- Doinikov, A. A., Haac, J. F., and Dayton, P. A. (2009). "Modeling of nonlinear viscous stress in encapsulating shells of lipid-coated contrast agent microbubbles," *Ultrasonics* **49**, 269–275.
- Erpelding, T. N., Hollman, K. W., and O'Donnell, M. (2005). "Bubble-based acoustic radiation force elasticity imaging," *Ultrason. Ferroelectr. Freq. Control. IEEE Trans.* **52**, 971–979.
- Fatemi, M., and Greenleaf, J. F. (1998). "Ultrasound-stimulated vibro-acoustic spectrography," *Science* **280**, 82–85.
- Field, S., and Drzewiecki, G. M. (1998). "Dynamic response of the collapsible blood vessel," in *Analysis and Assessment of Cardiovascular Function* (Springer, New York), pp. 277–296.
- Ilinskii, Y. A., Meegan, G. D., Zabolotskaya, E. A., and Emelianov, S. Y. (2005). "Gas bubble and solid sphere motion in elastic media in response to acoustic radiation force," *J. Acoust. Soc. Am.* **117**, 2338–2346.
- Karpouk, A. B., Aglyamov, S. R., Ilinskii, Y. A., Zabolotskaya, E. A., and Emelianov, S. Y. (2009). "Assessment of shear modulus of tissue using ultrasound radiation force acting on a spherical acoustic inhomogeneity," *IEEE Trans. Ultrason. Ferroelectr. Freq. Control* **56**, 2380–2387.
- Karshafian, R., Samac, S., Bevan, P. D., and Burns, P. N. (2010). "Microbubble mediated sonoporation of cells in suspension: Clonogenic viability and influence of molecular size on uptake," *Ultrasonics* **50**, 691–697.
- Koruk, H., and Choi, J. J. (2018). "Displacement of a bubble by acoustic radiation force into a fluid–tissue interface," *J. Acoust. Soc. Am.* **143**, 2535–2540.
- Koruk, H., El Ghamrawy, A., Pouliopoulos, A. N., and Choi, J. J. (2015). "Acoustic particle palpation for measuring tissue elasticity," *Appl. Phys. Lett.* **107**, 223701.
- Kruse, S. A., Smith, J. A., Lawrence, A. J., Dresner, M. A., Manduca, A., Greenleaf, J. F., and Ehman, R. L. (2000). "Tissue characterization using magnetic resonance elastography: Preliminary results," *Phys. Med. Biol.* **45**, 1579–1590.
- Kryuchkov, Y. N. (2001). "Concentration dependence of the mean interparticle distance in disperse systems," *Refract. Ind. Ceram.* **42**, 390–392.
- Lazarus, C., Pouliopoulos, A. N., Tinguely, M., and Garbin, V. (2017). "Clustering dynamics of microbubbles exposed to low-pressure 1-MHz ultrasound," *J. Acoust. Soc. Am.* **142**, 3135–3146.
- Leighton, T. G., Walton, A. J., and Pickworth, M. J. W. (1990). "Primary Bjerknes forces," *Eur. J. Phys.* **11**, 47–50.

- Maccabi, A., Shin, A., Namiri, N. K., Bajwa, N., John, M. S., Taylor, Z. D., Grundfest, W., and Saddik, G. N. (2018). "Quantitative characterization of viscoelastic behavior in tissue-mimicking phantoms and ex vivo animal tissues," *PLoS One* **13**, 1–18.
- Marmottant, P., van der Meer, S., Emmer, M., Versluis, M., de Jong, N., Hilgenfeldt, S., and Lohse, D. (2005). "A model for large amplitude oscillations of coated bubbles accounting for buckling and rupture," *J. Acoust. Soc. Am.* **118**, 3499–3505.
- Mettin, R., and Doinikov, A. A. (2009). "Translational instability of a spherical bubble in a standing ultrasound wave," *Appl. Acoust.* **70**, 1330–1339.
- Mikula, E., Hollman, K., Chai, D., Jester, J. V., and Juhasz, T. (2014). "Measurement of corneal elasticity with an acoustic radiation force elasticity microscope," *Ultrasound Med. Biol.* **40**, 1671–1679.
- Ophir, J., Céspedes, I., Ponnekanti, H., Yazdi, Y., and Li, X. (1991). "Elastography: A quantitative method for imaging the elasticity of biological tissues," *Ultrasound Imag.* **13**, 111–134.
- Postema, M., and Gilja, O. H. (2011). "Contrast-enhanced and targeted ultrasound," *World J. Gastroenterol.* **17**, 28–41.
- Pouliopoulos, A. N., Burgess, M. T., and Konofagou, E. E. (2018). "Pulse inversion enhances the passive mapping of microbubble-based ultrasound therapy," *Appl. Phys. Lett.* **113**, 044102.
- Prosperetti, A. (1987). "The equation of bubble dynamics in a compressible liquid," *Phys. Fluids* **30**, 3626–3628.
- Qiang, B., Greenleaf, J., Oyen, M., and Zhang, X. (2011). "Estimating material elasticity by spherical indentation load-relaxation tests on viscoelastic samples of finite thickness," *IEEE Trans. Ultrason. Ferroelectr. Freq. Control* **58**, 1418–1429.
- Saharkhiz, N., Koruk, H., and Choi, J. J. (2018). "The effects of ultrasound parameters and microbubble concentration on acoustic particle palpation," *J. Acoust. Soc. Am.* **144**, 796–805.
- Sarvazyan, A. P. (1975). "Low-frequency acoustic characteristics of biological tissues," *Polym. Mech.* **11**, 594–597.
- Sarvazyan, A. P., Rudenko, O. V., and Nyborg, W. L. (2010). "Biomedical applications of radiation force of ultrasound: Historical roots and physical basis," *Ultrasound Med. Biol.* **36**, 1379–1394.
- ter Haar, G. (2007). "Therapeutic applications of ultrasound," *Prog. Biophys. Mol. Biol.* **93**, 111–129.
- Urban, M. W., Nenadic, I. Z., Mitchell, S. A., Chen, S., and Greenleaf, J. F. (2011). "Generalized response of a sphere embedded in a viscoelastic medium excited by an ultrasonic radiation force," *J. Acoust. Soc. Am.* **130**, 1133–1141.
- Watanabe, T., and Kukita, Y. (1993). "Translational and radial motions of a bubble in an acoustic standing wave field," *Phys. Fluids A Fluid Dyn.* **5**, 2682–2688.
- Woodard, H. Q., and White, D. R. (1986). "The composition of body tissues," *Br. J. Radiol.* **59**, 1209–1218.
- Yang, X., and Church, C. C. (2005). "A model for the dynamics of gas bubbles in soft tissue," *J. Acoust. Soc. Am.* **118**, 3595–3606.
- Yoon, S., Aglyamov, S. R., Karpiouk, A. B., Kim, S., and Emelianov, S. Y. (2011). "Estimation of mechanical properties of a viscoelastic medium using a laser-induced microbubble interrogated by an acoustic radiation force," *J. Acoust. Soc. Am.* **130**, 2241–2248.
- Zabolotskaya, E. A., Ilinskii, Y. A., Meegan, G. D., and Hamilton, M. F. (2005). "Modifications of the equation for gas bubble dynamics in a soft elastic medium," *J. Acoust. Soc. Am.* **118**, 2173–2181.
- Zheng, H., Dayton, P. A., Caskey, C., Zhao, S., Qin, S., and Ferrara, K. W. (2007). "Ultrasound-driven microbubble oscillation and translation within small phantom vessels," *Ultrasound Med. Biol.* **33**, 1978–1987.
- Zhou, B., Sit, A. J., and Zhang, X. (2017). "Noninvasive measurement of wave speed of porcine cornea in ex vivo porcine eyes for various intraocular pressures," *Ultrasonics* **81**, 86–92.